Turkish Computational and Theoretical Chemistry

Turkish Comp Theo Chem (TC&TC)

Volume(Issue): 8(2) – Year: 2024 – Pages: 17-35

e-ISSN: 2602-3237

https://doi.org/10.33435/tcandtc.1372849

Received: 09.10.2023 ***Accepted:*** 04.02.2024 *Research Article*

DESIGN AND IN SILICO VALIDATION OF VITAMIN B5 AND ITS DERIVATIVES AS A POTENTIAL TARGET AGAINST CYCLOPHILIN A (CyPA)

Siddiq Jamal Sayeedha Tabassum[a,b], Predhanekar Mohamed Imran[a,1], Timiri Khudus Shabeer[c,2], Attar Kubaib [a], Ismail Salim Meeran [c]

[a] Department of Chemistry, Islamiah College (Autonomous), Vaniyambadi - 635752, Tamilnadu, India
[b] Department of Chemistry, Justice Basheer Ahmed Sayeed College for Women, Chennai – 600018, Tamilnadu, India
[c] Department of Chemistry, The New College, Chennai, Tamilnadu, India

Abstract: The title molecule N-(2,4-Dihydroxy-3,3-dimethylbutanoyl)-β-alanine or Vitamin B5 and its 23 derivatives were selected for theoretical investigations *viz* geometry optimization, ADME profiling, binding affinity using quantum-mechanical calculations and modeling simulation tools. Geometry optimization by Gaussian 09 program revealed the stability and electrophilic nature of the investigated molecules. In order to depict the charge density distributions, the contour maps of HOMO-LUMO and the associated chemical descriptors such as chemical potential (μ), electronegativity (χ), electrophilicity (ω), hardness (η) and softness (σ) were explored. The docked molecules showed strong propensity for binding to 2HQ6 cancer protein active sites. Vit B5-CH=CF_2 and Vit B5-CCl_3 showed low binding energies of -5.861 and -5.478 kcal/mol respectively with low inhibition constant value (1.43 M). The molecular docking and the druglikeness assessments were concomitant with the antiviral, antibacterial, and anticancer activities of the investigated molecules. Studies on the natural bond orbital (NBO), Mulliken population, and Fukui functions were analyzed. Further, the interactions between the derivatives and other molecules were studied using Hirshfeld surface analysis.

Keywords: Vitamin B5; Pantothenic acid; Coenzyme A; Quantum chemical descriptors; Molecular mechanics; DFT; drug likeness; ADMET; molecular docking; antiviral; antimicrobial; anticancer activity.

1. Introduction

Vitamins, including Vitamin B5 derivatives, display a comprehensive variety of biological and pharmacological properties. Vitamin B5, one of the potent water-soluble vitamins of the vitamin B complex, is also known commercially as D-pantothenic acid or pantothenate. Since pantothenic acid is present in almost all foods, the word "pantothenic" is derived from the Greek word "pantou", which means "everywhere". Vitamin B5 is present in all sources of plants and animals. For the formation of coenzyme-A (CoA), as well as for the metabolization of carbohydrates, proteins, and lipids, animals need pantothenic acid [1].

In the year 1933, an American biochemist Roger John Williams discovered Vitamin B5 or pantothenic acid whose structure as shown in Figure 1. Vitamin B5 is a precursor of coenzyme A (CoA), involved in various enzymatic pathways in the body. It plays a crucial role in the conversion of energy for many biological functions and in the conversion of the various other B vitamins into forms which is acceptable by the body. Pantothenic acid is a potent antioxidant and a neural compound which helps in boosting the immune system and neural functions. It also aids in metabolising fat and reducing stress levels [2].

Under physiological circumstances, pantothenic acid is negatively charged and soluble in water (log P= 1.69). When the pH is low (between 2 and 3), it has no charge [3]. Because of its relative instability, pantothenic acid decomposes chemically quickly in both acidic and basic environments. Additionally, heat accelerates the breakdown of pantothenic acid

[1]Corresponding Authors e-mail: imranpkm@gmail.com

[2]Corresponding Authors e-mail: shabeer@thenewcollege.edu.in

[4]. There is no proof that exposure to light affects pantothenic acid's stability. Table 1 displays the biophysical characteristics of vitamin B5. For the creation of brand-new antiviral, antibacterial, and anticancer drugs, the pre-selected compounds could be promoted as promising drug candidates.

Table 1. Biophysical Properties of Vitamin B5

Molecular weight	219.24 g//mol
Estimated log P	− 1.69
Solubility	Freely soluble in water, ethyl acetate, dioxane, glacial acetic acid Moderately soluble in ether, amyl alcohol Practically insoluble in benzene and chloroform

The B-series vitamins (B1 to B6 and B11) have been intensively investigated with regard to their anticancer behaviour and strongly expressed synergistic effect on cytostatic agents. Vitamin B5 occurs in all animal and plant tissues, however, the richest source is the jelly of the queen bee and liver. Vitamin B5 and its derivatives have versatile biological properties. Among its antioxidant actions [5,6] it exhibits protective ability against ionizing radiations [7,8], which is mainly referred to OH-radicals [9] ($k=4.5\times109$ $L.mol^{-1}.s^{-1}$). Vitamin B5 exhibits an essential anticancer effect in *in-vitro* tests, according to a recent report [10]. Vitamin B5 demonstrates rather high antitumor effect in different media. The products resulting from the attack of free radicals ($OH^{\cdot}$) on Vitamin B5 are very likely involved in the observed anticancer effect.

Despite advances in anticancer therapeutic interventions, the majority of anticancer drugs continue to face multiple challenges. The present-day lifestyle has caused the emergence of increased number of cancer cases requiring the quest for novel chemical utilities to address these deficiencies in anticancer treatment. The efficacy of such Vitamin B5 and their derivatives has prompted chemists to synthesize efficient novel drugs to satisfy the demands of the world's growing health problems.

Computational approaches to drug discovery and design have increased in popularity due to its reliability in discovering molecules with high pharmacological properties [11]. The molecular docking technique is frequently used to evaluate the binding affinity of drug molecules and to determine the correct orientation of drug molecules in the protein-active site [12,13]. Other virtual screening approaches for the adoption of compounds that display physiological activities and drug-like identities include drug similarity criteria and an *in-silico* ADMET profile based on their drug database model [14,15]. For several material systems, density functional theory (DFT) calculations produce the most accurate and trustworthy results that are quite consistent with the experimental data [16,17]. In this research work, DFT calculations, ADMET, Hirshfeld analysis and molecular docking studies were used to provide a systematic computational analysis of Vitamin B5 and 21 of its virtually modified derivatives in Figure 1.

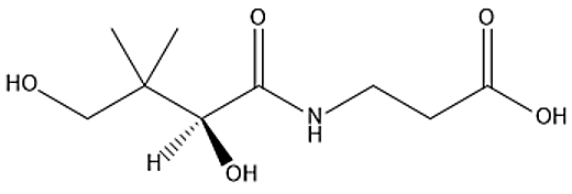

a.i.

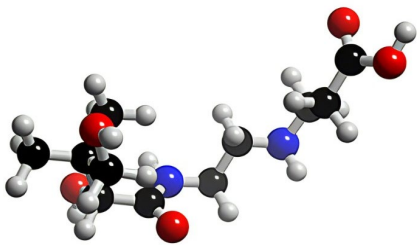

ii.

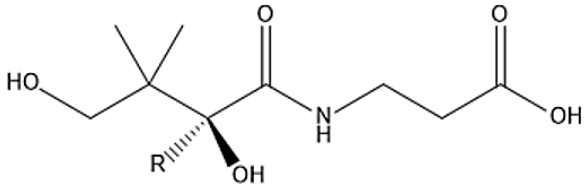

b.

R= H, CH_3, CH_2Cl, CCl_3, CH_2F, CHF_2, CF_3, $CH{=}CH_2$, $CH{=}CHF$, $CH{=}CF_2$, CH_2CN, CH_2NCO, CH_2OH, CH_2CONH_2, CH_2NCS, CPF, CPF_2, OCF_3, OCH_2F, OCH_3, $OCHF_2$,
CP – Cyclopropan

Figure 1. a. i. Molecular structure & ii. Optimized structure of Vitamin B5 (Pantothenic acid), b. Virtually modified derivatives of Vitamin B5

2. METHOD

2.1. Selection of target protein

Cyclophilin-A (CyPA): A crucial component in human disease

The immunophilin family of proteins includes the widely dispersed cyclophilin A (CyPA) Figure 2. Peptidyl prolyl cis-trans isomerase (PPIase) activity, which is present in CyPA, controls the folding and transport of proteins. CyPA can be released by cells in response to inflammatory stimuli. CyPA plays a crucial role of in a number of human disorders has been strongly supported by recent studies in both human and animal models [18].

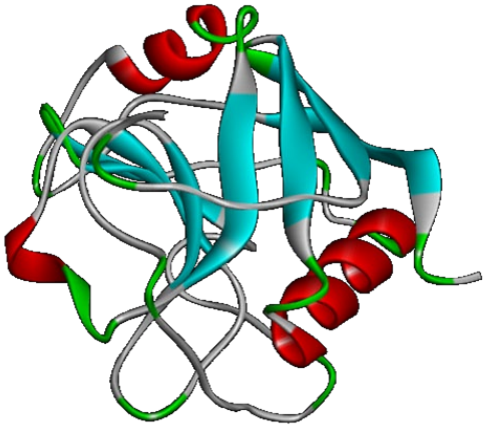

Figure 2. Ribbon diagram of Cyclophilin A (CyPA)

Influenza A virus and CyPA.

According to Liu et al [19], while overexpressing CyPA reduced influenza A viral replication, decreasing endogenous CyPA increased the production of the virus. Furthermore, CyPA interacts with (M1) matrix protein 1 and influences the early stages of viral transmission. Finally, CyPA restricted influenza virus growth by accelerating the degradation of the protein M1. Through its incorporation into particles [20] and binding to the nucleocapsid protein, CyPA has also been implicated in controlling the replication of the SARS-CoV coronavirus.

Protozoan Parasites

A growing body of research indicates the significance of CyPA in the development of human parasitic protozoa. Mammalian CyPA host cell is involved in the replication cycle of intracellular Leishmania major parasites [21]. The participation of CyPA in protozoan parasite development was further supported by the finding of anti-parasitic activity of CsA against a wide range of parasites [22] with the exclusion of Leishmania [23]. Some of the minor CyPs from Toxoplasma gondii and Plasmodium falciparum (i.e. TgCyP18) have shown similar inhibitory profiles to those established for the human CyPA [24,25].

CyPA and Cancer Upregulation of CyPA

The function of CyPA in cancer is now a well-established field of study. Indeed, numerous studies have established that CyPA is increased in cancer and is a vital part in the development of metastasis and malignant transformation [26,27]. In small cell lung cancer, CyPA overexpression promotes cancer cell proliferation [28] while CyPA knockdown inhibits it. CyPA participates in several pathogenic processes that lead to the development of cancer. In particular, it has been noted that CyPA is overexpressed in several cancers: (1) aids in cancer proliferation [29]; (2) controls cell cycle progression [30]; (3) inhibits apoptosis [31]; and (4) encourages cell migration/invasion [32]. Remarkably, chemotherapeutic agents influence the expression of CyPA. Treatment, for example with anti-cancer medications such as 5-aza-2-deoxycytidine, celecoxib, and 5-fluorouracil, reduces the expression of CyPA in cancer cells [33, 34]. Moreover, CsA and sanglifehrin A (SfA), the

two immunosuppressive drugs that bind CyPA, increase the chemotherapeutical outcome of cisplatin in glioblastoma multiforme [35]. Given CyPA's critical role in controlling the replication and infectivity of many viruses, it is worthwhile to suggest CyPA as a target for our biological evaluation.

3. Methodology and Computational details

The Becke-3 Parameter-Lee-Yang-Parr (B3LYP) and 6-311G basis set model of the DFT method [36, 37], was utilised to employ the Gaussian 09 software suite to optimize the title molecule [38]. The output data was analysed using the Gauss View 5.0 graphical user interface, including the optimised geometry, HOMO-LUMO and MEP [39]. According to DFT, the first and second partial derivatives of a system are its chemical potential (μ) and global hardness (η), respectively in relation to the quantity of electrons (N) at a certain external potential, v(r). Electronegativity (χ), is finitely identical with the definition of the chemical potential, which is expressed as [40];

$$\chi = -\frac{dE}{dN}$$

This can be written as,

$$\chi = \frac{IP+EA}{2}$$

where IP denotes the first ionisation potential and EA denotes the first electron affinity. The comparable second derivative of E(N) with respect to N, while maintaining a constant external potential (v) or nuclear charge, is the absolute hardness [41].

$$\eta = \frac{1}{2}\left(\frac{\partial^2 E}{\partial N^2}\right)$$

From the above equation, hardness can be related to electronegativity or chemical potential as,

$$2\eta = \left(\frac{\partial \mu}{\partial N}\right)_v = -\left(\frac{\partial \chi}{\partial N}\right)_v$$

The reverse of the hardness has been known as the softness.

$$S = \frac{1}{2}\eta = \left(\frac{\partial N}{\partial \mu}\right)_v$$

The system's overall stability is indicated by its global softness (S). The ionisation potential and electron affinity can be used to represent the chemical potential or electronegativity and hardness [42]. The difference between the right and left derivatives is then used to express the finite-difference approximation to the second order energy derivative ($\partial^2 E/\partial N^2$). As a result, and can be expressed as,

$$\mu = \frac{-(IP+EA)}{2}$$

$$\eta = \frac{(IP-EA)}{2}$$

The above-mentioned quantities are represented by frontier orbital energies. They can be calculated using the Koopmans' approximation within Molecular Orbital (MO) theory, in which the Ionisation Potential (IP) and Electron Activity (EA) are related to HOMO and LUMO energy as,

$$-E_{HOMO} = IP$$

$$-E_{LUMO} = EA$$

Hence, μ and η can be written in terms of HOMO and LUMO as

$$\mu = \frac{(E_{LUMO}+E_{HOMO})}{2}$$

$$\eta = \frac{(E_{LUMO}-E_{HOMO})}{2}$$

$$\sigma = 1/\eta$$

$$\omega = \chi^2/2\eta$$

FMO predicts that an electrophilic reaction will occur in a molecule at a location with a high relative density of HOMO, and that a nucleophilic reaction will occur preferentially at a location with a high relative density of LUMO. The site selectivity and reactivity of atoms in all systems have been extensively studied using reactivity descriptors. The global reactivity descriptors were evaluated using the DFT method using basis set 6-311G (d,p). For the parameters of the descriptors, Koopman's method was used.

Auto Dock Tools 1.5.6 [43] was used to obtain the binding affinities and types of interactions between the ligand and target proteins for molecular docking computation. The X-ray crystal structure of peptidyl prolyl cis-trans isomerase (PPIase) of CyPA (PDB code: 2HQ6) was downloaded from the protein data bank (http://www.rcsb.org./pdb). 2HQ6 was the structure of cyclophilin-like domain of the serologically defined colon cancer. The protein was prepared for docking by deleting the water molecules, merging polar hydrogen atoms and adding Kollman charges. Gasteiger charges were computed and the non-rotatable amide bonds were made to rotate. The protein was bounded in a grid box with dimensions of 90 × 90 × 90 grid points along x × y × z directions with 0.370 Å spacing and Lamarckian genetic algorithm was employed to perform the docking calculations. The output file in 'dlg' format provided the key information about the binding energies of the various docked conformations.

The Discovery Studio 4.5 programme was used to display the ligand-protein interactions [44]. Swiss ADME, an open-source online server was used to evaluate the ADMET properties of the drug candidates [45].

4. Results and discussion

4.1. Frontier Molecular Orbitals

Frontier molecular orbitals (FMO's) are used to predict and explain many types of reactions as well as the most reactive locations in molecular systems. LUMO and HOMO orbitals, are very helpful for characterizing materials to understand the chemically reactivity of the molecules [46]. Since the HOMO orbital has a high electron density, it frequently transfers electrons to open orbitals. On the other hand, LUMO is an empty orbital that can readily take electrons from other filled orbitals. Vit B5 CH=CF_2 displayed lowest energy gap of 2.26 eV and thus expected to show better biological activities.

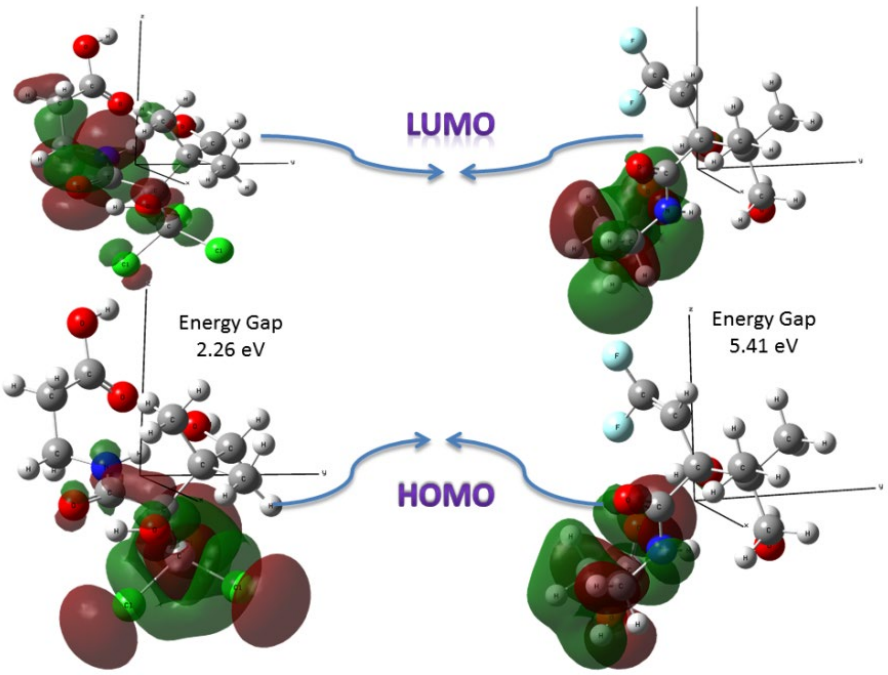

Figure 3. HOMO-LUMO contour maps for Vit B5 CH=CF_2 and Vit B5 CCl_3

4.2. Quantum Chemical Descriptors

In the context of quantum chemical calculations, the study of electronic energies has become important in better understanding the nature of molecular chemical stability and reactivity. A theoretical method for connecting the chemical activities of molecular structures to their electrical characteristics is represented by Koopmans' theorem [47]. Quantum chemical descriptors derived from Koopman's theorem are used to evaluate parameters such as electron affinity (A), ionization potential (I), hardness (η), softness (σ), chemical potential (μ), electronegativity (χ), and electrophilicity (ω) to predict a molecule's reactivity are given in Table 2. Vit B5 CH=CF_2 showed the lowest hardness value of 1.13 attributed to the presence of two fluorine atoms and thus said to possess high chemical stability.

Table 2. Various substituents and molecular descriptors of the Vitamin B5 derivatives

S.No	R	Energy Band Gap (ΔE) in eV	Global Hardness (η)	Global Softness (1/ή)	Electro-negativity (χ)	Chemical Potential (μ)	Global Electro-philicity (ω)
1	H	5.82	2.91	0.34	4.16	-4.16	2.98
2	CH_3	5.52	2.76	0.36	4.09	-4.09	3.03
3	CH_2Cl	5.90	2.95	0.34	4.34	-4.34	3.19
4	$CHCl_2$	5.98	2.99	0.33	4.46	-4.46	3.33
5	CCl_3	5.41	2.71	0.37	4.64	-4.64	3.97
6	CH_2F	5.68	2.84	0.35	4.04	-4.04	2.87

7	CHF_2	6.01	3.01	0.33	4.42	-4.42	3.25
8	CF_3	6.45	3.22	0.31	4.15	-4.15	2.67
9	$CH{=}CH_2$	5.85	2.92	0.34	4.04	-4.04	2.79
10	CH=CHF	6.01	3.01	0.33	3.96	-3.96	2.61
11	$CH{=}CF_2$	2.26	1.13	0.89	4.20	-4.20	7.82
12	CH_2CN	5.90	2.95	0.34	3.90	-3.90	2.58
13	CH_2NCO	6.50	3.25	0.31	3.82	-3.82	2.25
14	CH_2OH	5.63	2.82	0.36	4.18	-4.18	3.10
15	CH_2CONH_2	5.68	2.84	0.35	4.04	-4.04	2.87
16	CH_2NCS	6.23	3.11	0.32	4.01	-4.01	2.58
17	CPF	5.82	2.91	0.34	4.03	-4.03	2.78
18	CPF_2	5.82	2.91	0.34	4.13	-4.13	2.94
19	OCF_3	5.74	2.87	0.35	4.39	-4.39	3.36
20	OCH_2F	5.66	2.83	0.35	4.19	-4.19	3.10
21	OCH_3	5.49	2.75	0.36	4.05	-4.05	2.99
22	$OCHF_2$	14.47	7.24	0.14	3.70	-3.70	0.95
23	CP	5.63	2.82	0.36	3.93	-3.93	2.74
24	CH_2SH	5.11	2.56	0.39	3.86	-3.86	2.92

Table 3. Top-five Vitamin B5 derivatives with better FMO and molecular descriptor values

R	E HOMO (eV)	E LUMO (eV)	Energy Band Gap	Global Hardness (η)	Global Softness (1/η)
$CH{=}CF_2$	-5.33	-3.07	2.26	1.12	0.88
CH_2SH	-6.41	-1.30	5.11	2.55	0.39
CCl_3	-7.34	-1.93	5.41	2.70	0.36
OCH_3	-6.80	-1.30	5.49	2.74	0.36
CH_3	-6.85	-1.33	5.52	2.76	0.36

Table 4. Binding Energy Values from Molecular Docking Results

S.No	R	Binding Energy kJ/mol
Ligand A	$CH{=}CF_2$	-5.861
Ligand B	CH_2SH	-1.355
Ligand C	CCl_3	-5.478
Ligand D	OCH_3	-2.159
Ligand E	CH_3	-2.395

3.1.Molecular Docking

From the global softness values the top five Vitamin B5 derivatives were selected for ADMET studies and molecular docking as mentioned in Table 3. Using Auto Dock software, the behaviour of derivatives of vitamin B5 in the functional sites of receptor 2HQ6 protein was investigated. Binding energy affinity is considered to be an important predictor to assess the biological activities. The active site of the cyclophilin family includes the invariant catalytic arginine (Arg55) and a highly conserved mixture of hydrophobic, aromatic, and polar residues including Phe60, Met61, Gln63, Ala101, Phe113, Trp121, Leu122, and His126. All of these side chains contribute to an extensive binding surface along one face of the PPIase domain measuring roughly 10 Å along the Arg55–His126 axis and 15 Å along the Trp121–Ala101 axis [48]. The selected compounds (listed in Table 3) were docked with the active site of 2HQ6, and the binding energies of the docked molecules were examined to determine a minimal value.

The results (Table 4) show the binding energy values of the docked ligands. Ligand A exhibited 4 H/O hydrogen bonding interactions with Gln64, Gln112, Gly72, Gly110, Ala102 and one H/N hydrogen bonding interaction with Gln112, with RMSD value being 0.003A˚. Ligand C exhibited 5 H/O hydrogen bonding interactions with Ala102, Gly110, Gly72, Gln72, Asn103 and a H/N hydrogen bonding with Gln72 with RMSD being 0.013 A˚ as mentioned in Figure 5. Binding affinities of the potent CypA inhibitors were

ranging from 5.3 Kcal/mol and -7.5 Kcal/mol [49]. The results of the molecular docking analysis indicated that ligand A (Vit B5-CH=CF_2) and ligand C (Vit B5-CCl_3) have the lowest binding energies, with -5.861 and -5.478 kcal/mol, respectively comparable with that of the CypA inhibitors. Consequently, these Vitamin B5 derivatives possess beneficial biological activities, including antiviral, antibacterial, and anticancer properties.

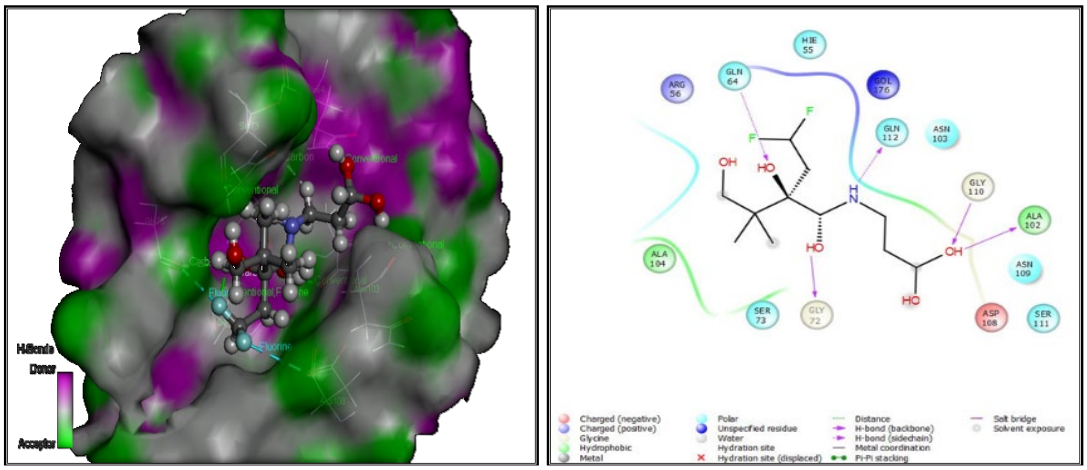

Figure 4. Docking pose and 2D interaction of Vit B5 CH=CF_2 with 2HQ6

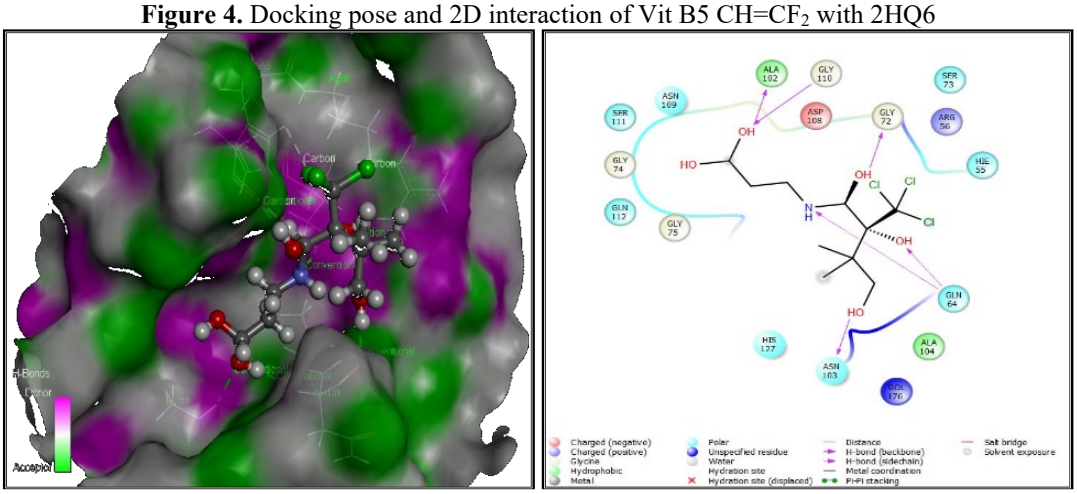

Figure 5. Docking pose and 2D interaction of Vit B5 CCl_3 with 2HQ6

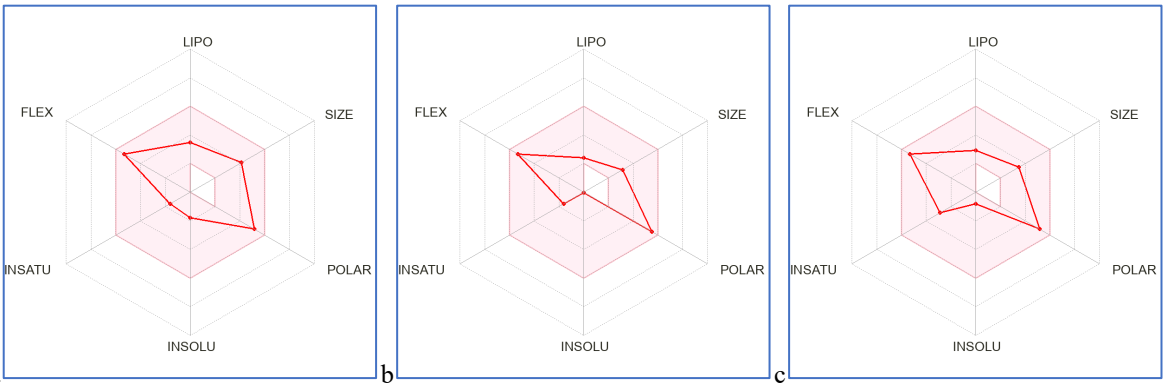

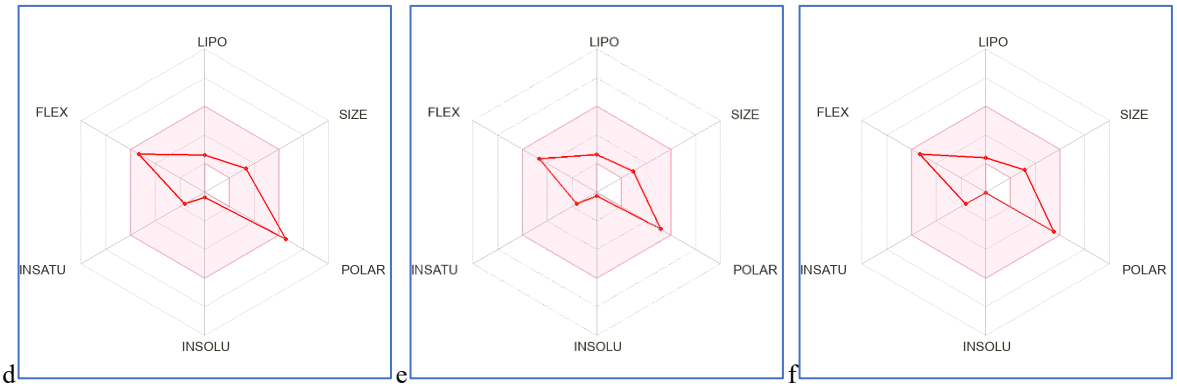

Figure 6. Bioavailability radar plots of (a). Vit B5, (b). Vit B5-CCl3, (c). Vit B5- $CH{=}CF_2$, (d). Vit B5-CH_2SH, (e). Vit B5- CH_3, (f). Vit B5- OCH_3

Table 5a. ADMET parameters of Vitamin B5 derivatives

Ligand	MW	Donor HB	Acceptor nHB	logP
Vit-B5	219.23	4	5	-0.48
Vit-B5-CCl_3	336.6	4	5	0.86
Vit-B5-$CH{=}CF_2$	281.25	4	7	0.43
Vit-B5-CH_2SH	265.33	4	5	-0.17
Vit-B5-CH_3	233.26	4	5	-0.26
Vit-B5-OCH_3	249.26	4	6	-0.5
Recommended values	≤500	≤5	≤10	≤5

Table 5b. ADMET parameters of Vitamin B5 derivatives

Ligand	RBC	Rule of five	TPSA(Å 2)	Bioavailability Score
Vit-B5	7	0	106.86	0.56
Vit-B5-CCl_3	8	0	106.86	0.56
Vit-B5-$CH{=}CF_2$	8	0	106.86	0.56
Vit-B5-CH_2SH	8	0	145.66	0.56
Vit-B5-CH_3	7	0	106.86	0.56
Vit-B5-OCH_3	8	0	116.09	0.56
Recommended values	≤10	Max 2	≤140	

Abbreviations: MW- Molecule's molecular weight, donor HB stands for the approximation of the number of hydrogen bonds the solute would donate to water molecules in an aqueous solution, accept HB stands for the approximation of the number of hydrogen bonds the solute would take away from water molecules in an aqueous solution.

Table 6. Lipinski rule parameters of Vitamin B5 derivatives

Ligand	Log S	Solubility	LogKp (cm/s)	GI Absorption	BBB Permeability	Pgp substrate
Vit-B5	-0.67	High soluble	-8.4	High	No	No
Vit-B5-CCl_3	-2.42	Soluble	-7.93	High	No	No
Vit-B5-$CH{=}CF_2$	-1.4	High soluble	-8.29	High	No	No
Vit-B5-CH_2SH	-1.61	High soluble	-8.6	Low	No	No
Vit-B5-CH_3	-0.87	High soluble	-8.35	High	No	No
Vit-B5-OCH_3	-0.64	High soluble	-8.74	High	No	No

3.4. Drug Likeness and ADMET Assessment

A medicine's physicochemical properties are related to the required biopharmaceutical properties in the human body to determine its "drug similarity." ADMET stands for absorption, distribution, metabolism, excretion and toxicity properties of a drug. Lipinski's rule of five, and drug likeness provide the benchmark for a drug

candidate to be considered as a good drug [50]. The rules are: molecular weight < 500, (octanol/water coefficient) logP ≤ 5, hydrogen bond donors HBD ≤ 5, hydrogen bond acceptors ≤ 10 [51,52]. Tables 5a, 5b and 6 show that the Vitamin B5 and its selected derivatives possess optimal ADMET properties and obeys Lipinski's rule of five with zero violation and thus has the potential to be used as good therapeutic candidates. The bioavailaility radar plot (figure 6) displays the druglikeness of the drug candidates. The plots shows that all the 6 candidates have the optimal range of all the six properties, and hence can be considered to possess significant therapeutic potentials.

The Brain Or Intestinal EstimateD permeation method (BOILED-Egg) accurately predicts the passive human gastrointestinal absorption (HIA) and brain permeability (BBB) of a drug. This model depend on WLOGP and TPSA descriptors for assessing the lipophilicity and corresponding polarity [53]. Figure 7 shows the BOILED-egg model of vitamin B5 and its derivatives. Except molecule 4 (Vit-B5-CH_2SH), all other molecules were spotted in the white yolk attributed to highly probable HIA absorption. The ligands under study have high intestinal absorbance, indicating their ease of absorption.

Solubility is a significant condition in achieving the optimum pharmacological drug. Low solubility is the major issue experienced when synthesizing novel drugs. The calculated water solubility values as mentioned in the Table 6 classify the studied molecules as highly soluble drugs and hence having desired pharmacokinetics property for absorption and distribution [54]. Lower the Log Kp value, the more challenging for the epidermis to absorb the subject molecule [55]. One of the earliest ABC transporter members, P-glycoprotein (P-gp) serves as a physiological barrier by pushing xenobiotics and poisons out from the cells [56, 57]. The apical surface of the epithelial cells lining the small intestine, colon, bile ductules, pancreatic ductules, kidney proximal tubules, and adrenal gland is where P-gp is primarily found [58, 59]. It is also located in the endothelial cells of the blood brain barrier (BBB) [60]. The transporter is overexpressed on the surface of many neoplastic cells and restricts cell entry. P- gp's is likely to shield these vulnerable organs from hazardous substances by inhibiting their entry into the cytosol and expulsion to the outside [61]. Thus, it also enhances the secretion of metabolites and xenobiotics into bile, urine, and the lumen of gastrointestinal tract.

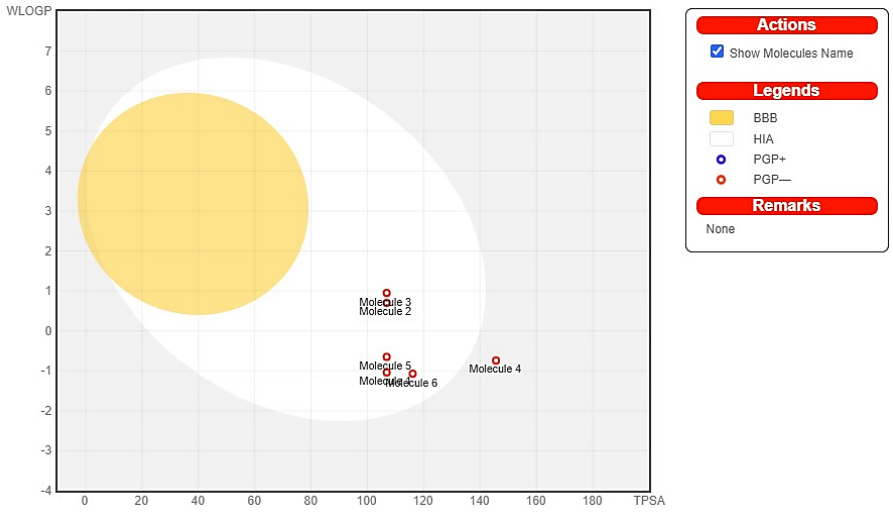

Molecule 1: Vit B5, Molecule 2: Vit B5-CCl3, Molecule 3: Vit B5-CH=CF_2, Molecule 4: Vit B5-CH_2SH, Molecule 5: Vit B5-CH_3, Molecule 6: Vit B5-OCH_3

Figure 7. Boiled Egg Model of Vitamin B5 and its derivatives

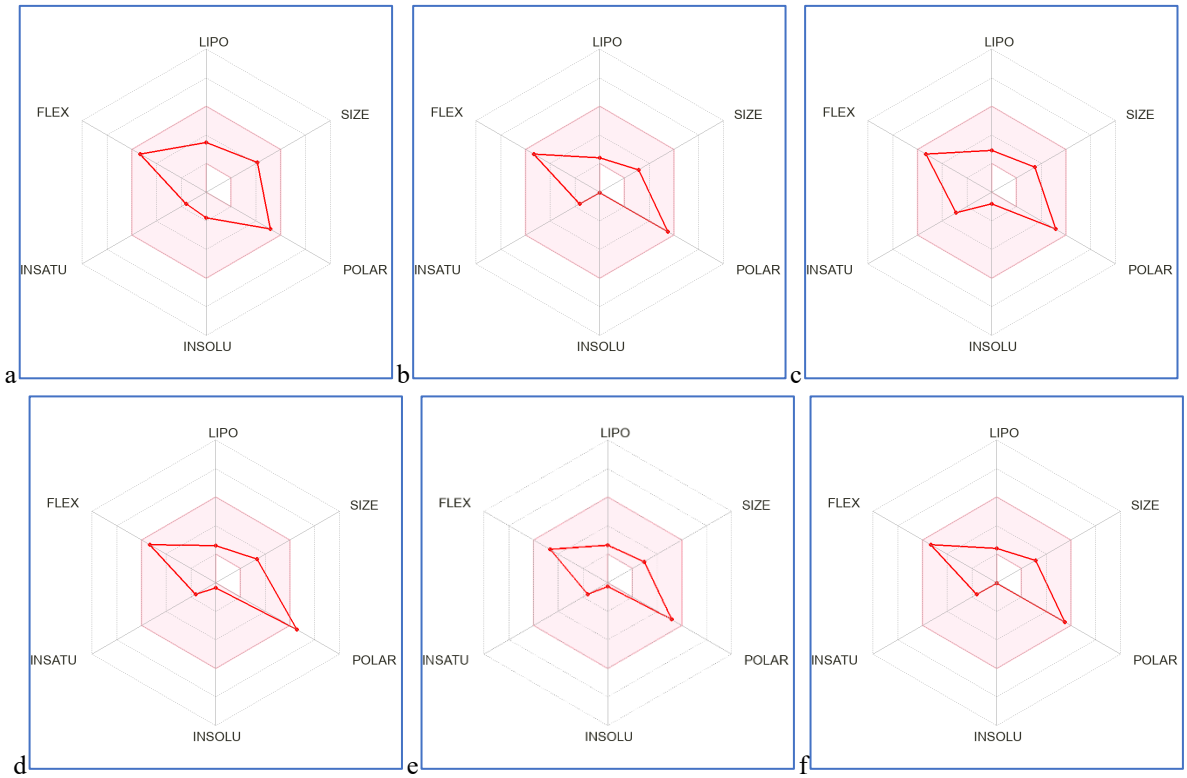

Figure 7. Bioavailability radar plots of (a). Vit B5, (b). Vit B5-CCl3, (c). Vit B5- $CH=CF_2$, (d). Vit B5- CH_2SH, (e). Vit B5- CH_3, (f). Vit B5- OCH_3

3.5.Molecular electrostatic potential (MEP) and Hirshfeld surface (HS) analysis

Hirshfeld surfaces' maps of electrostatic potential make available precise information on the interactions between molecules in crystals [62]. MEP is used to discover the electrophilic and nucleophilic attacks during the reactions as well as hydrogen bonding interactions. Figures 8 and 9 show the MEP map of Vit B5-CCl_3, ranges from -7.2 a. u (deepest red) to 7.2 a.u (deepest blue) and of Vit B5-$CH=CF_2$ ranges from -7.43 a.u (deepest red) to 7.43 a.u (deepest blue). Besides, the positive potential and the negative potential are represented by blue and red colours, respectively. The negative electrostatic potential is generally incorporated with the lone pair of electronegative atoms.

Hirshfeld surfaces gives, the molecular surface analysis, electrostatic potential, di, de, dnorm, shape index and curvedness, for Vit B5 CCl_3 and Vit B5 $CH=CF_2$ molecules as shown in Figures 10(a-f) & 11(a-f) respectively. The dnorm surface (Figures 10d & 11d) is a normalized contact distance, ranging from [0.3193 Å (red) to 6.2907 Å (blue)] for Vit B5 CCl_3 & [-0.2627 Å (red) to 7.1076 Å (blue)] for Vit B5 $CH=CF_2$. The positive dnorm value is represented by red colour regions with longer intermolecular interactions, the negative dnorm value is indicated by blue colour regions with shorter intermolecular contacts, and the zero dnorm value is indicated by white colour region. The de surface of Figures 10c & 11c show the distance between the nearest nuclei external to the surface region of Vit B5 CCl_3 (1.4068–7.0505 Å) & Vit B5 $CH=CF_2$ (0.9768-7.6058 Å). The shape index surface (Figures 10e & 11e) show the electron density surface curves around the molecular interaction range from (-1 Å to 1 Å) for both the derivatives [63, 64]. The curvedness (Figures 10f & 11f) indicates the electron density surface curves around the molecular interaction range (-4 Å to 0.4 Å) for both the derivatives respectively.

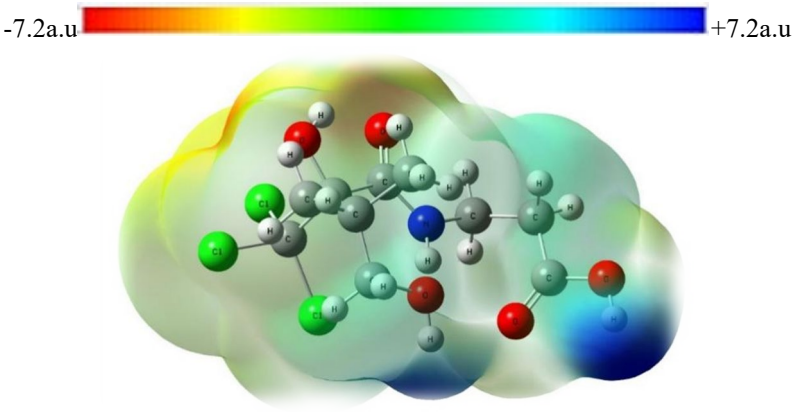

Figure 8. MEP of Vit B5 CCl_3

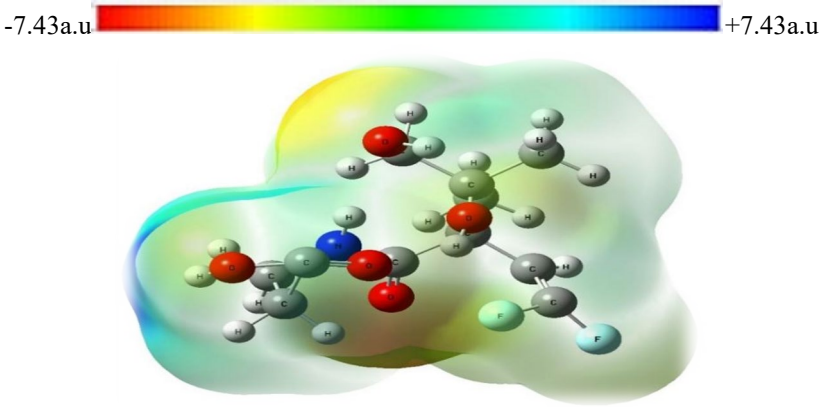

Figure 9. MEP of Vit B5 $CH=CF_2$.

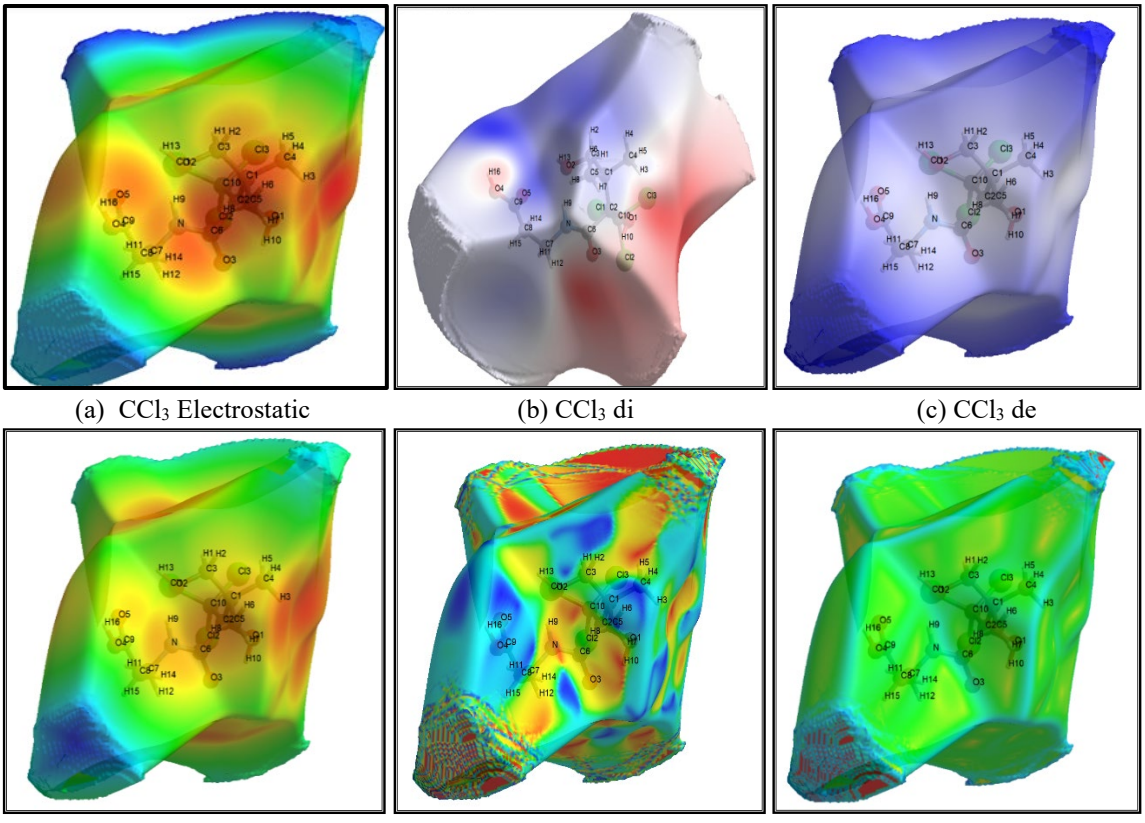

(a) CCl_3 Electrostatic (b) CCl_3 di (c) CCl_3 de

(d) CCl_3 dnorm (e) CCl_3 shape index (f) CCl_3 curvedness

Figure 10. Molecular surface analysis of Vit B5 CCl_3

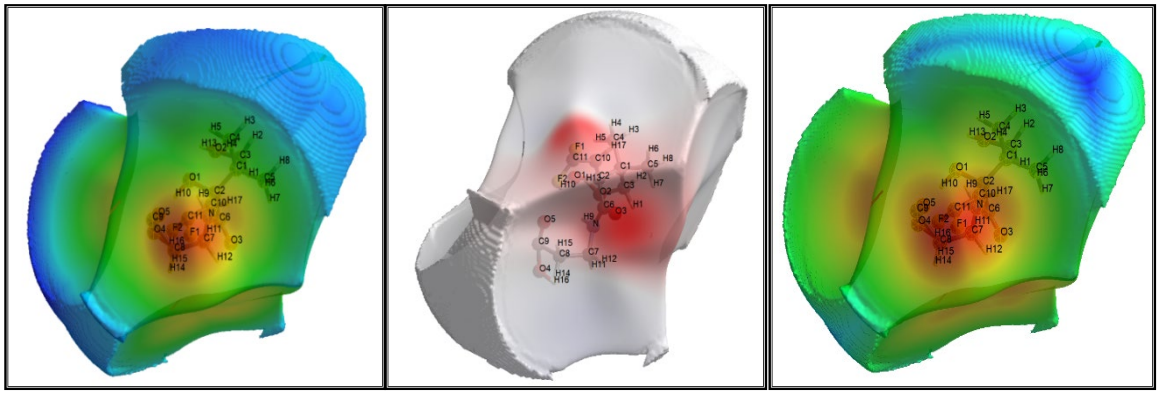

a. CH=CF_2 Electrostatic b. CH=CF_2 di c. CH=CF_2 de

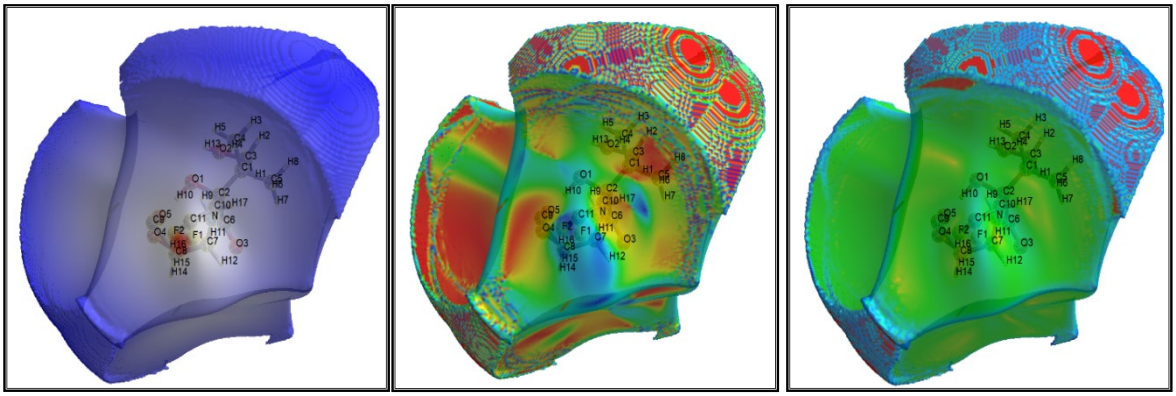

d. CH=CF_2 Norm e. CH=CF_2 shape index f. CH=CF_2 curvedness

Figure 11. Molecular surface analysis of Vit B5 CH=CF_2

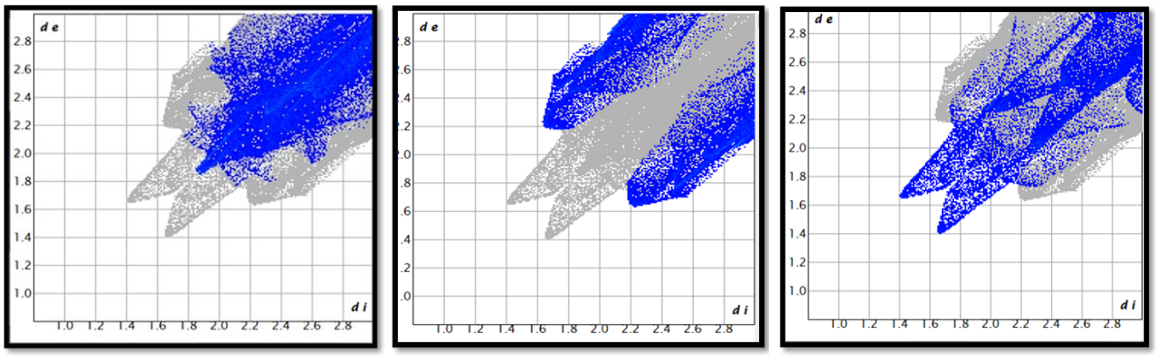

H-H 39.4% H-Cl -34.4% H-O -16.4%

Figure 12. Finger Print Plots of Vitamin B5 CCl_3

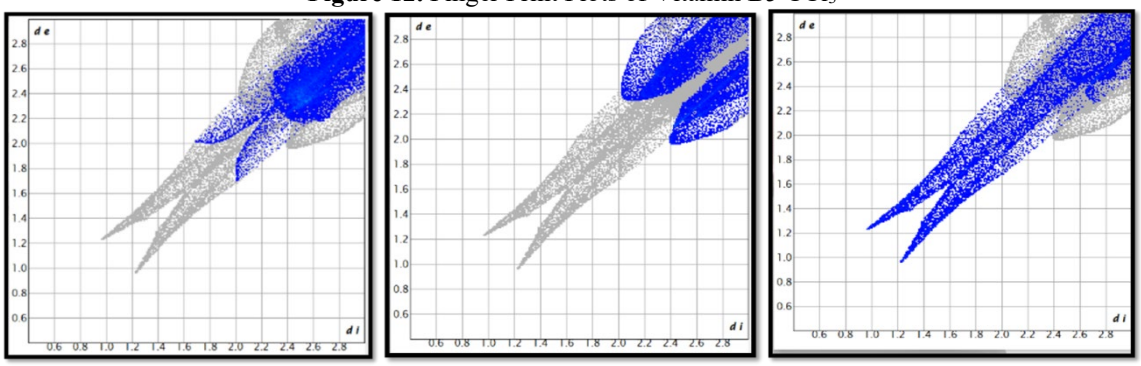

H-H – 39.1% H-O 24.1% H-F-19.1%

Figure 13. Finger Print Plots of Vitamin B5 CH=CF_2

Figure 12 illustrates the plot of the 2D fingerprint for Vit B5 CCl_3 that was resolved into H---H, H---O, and H---Cl contacts, along with the interaction percentages and their proportional contributions. H---H (39.4%) and H---O (16.4 %) are the largest and minimum contributions, respectively. The outcome confirms that the super-molecular property of the Vit B5 CCl_3 molecule. Figure 13 illustrates the plot of the 2D fingerprint for Vit B5 $CH=CF_2$ that was resolved into H---H, H---O, and H---F contacts, along with the interaction percentages and their proportional contributions. H----H (39.1%) and H---O (19.1%) are the largest and minimum contributions, respectively. The outcome confirms that the super-molecular property of the Vit B5 $CH=CF_2$ molecule.

3.6.Donor- Acceptor Interactions

4.The most effective way to describe charge transfer, conjugative interactions, intramolecular-intermolecular bonding, and stabilisation energy in a molecular system is through the NBO analysis [65]. This analysis has been done on the Vitamin B5 derivatives and is listed in Table 7 & 8. The NBO analysis is performed to find the electron donor-electron acceptor interaction energy in the Vitamin B5 derivatives. The second order Fock matrix was finalized to calculate the donor-acceptor interactions in the NBO analysis. The stabilization energy E (2) for each electron-donor (i) and electron-acceptor (j) were done.

Table 7. Fukui function parameters of Vit B5 CCl_3.

N	Z	f-	f+	f0	Dual-Descrpt	Hardness (au)	W-(eV)	W+(eV)
1	8	0.0001	0	0	0	0	0	0
2	8	0.0001	0	0.0001	-0.0001	0	0.0001	0
3	8	0.0003	0	0.0002	-0.0003	0.0001	0.0003	0
4	8	0.0001	0.008	0.004	0.0079	0	0.0001	0.0075
5	8	0.0001	0.3407	0.1704	0.3407	-0.0027	0.0001	0.3181
6	7	0.9623	0.0005	0.4814	-0.9619	0.24	0.8983	0.0004
7	6	0.0009	0	0.0005	-0.0009	0.0002	0.0009	0
8	6	0.0008	0.0004	0.0006	-0.0004	0.0002	0.0008	0.0004
9	6	0	0	0	0	0	0	0
10	6	0	0	0	0	0	0	0
11	6	0.0003	0	0.0001	-0.0002	0.0001	0.0002	0
12	6	0.0191	0.0003	0.0097	-0.0188	0.0048	0.0178	0.0003
13	6	0.013	0.0019	0.0074	-0.0111	0.0032	0.0121	0.0017
14	6	0.0011	0.0056	0.0033	0.0045	0.0002	0.001	0.0052
15	6	0.0008	0.6411	0.321	0.6404	-0.0049	0.0007	0.5985
16	6	0.0002	0	0.0001	-0.0002	0.0001	0.0002	0
17	1	0	0	0	0	0	0	0
18	1	0	0	0	0	0	0	0
19	1	0	0	0	0	0	0	0
20	1	0	0	0	0	0	0	0
21	1	0	0	0	0	0	0	0
22	1	0	0	0	0	0	0	0
23	1	0	0	0	0	0	0	0
24	1	0.0001	0	0.0001	-0.0001	0	0.0001	0
25	1	0.0001	0.0001	0.0001	-0.0001	0	0.0001	0.0001
26	1	0	0	0	0	0	0	0
27	1	0	0.0003	0.0002	0.0003	0	0	0.0003
28	1	0	0	0	0	0	0	0

29	1	0	0	0	0	0	0	0
30	1	0.0001	0.0006	0.0004	0.0005	0	0.0001	0.0006
31	1	0	0.0004	0.0002	0.0004	0	0	0.0004
32	1	0	0	0	0	0	0	0
33	17	0.0003	0	0.0002	-0.0003	0.0001	0.0003	0
34	17	0	0	0	0	0	0	0
35	17	0	0	0	0	0	0	0

Table 8. Fukui function parameters of Vit B5 $CH=CF_2$.

N	Z	f-	f+	f0	Dual-Descrpt	Hardness (au)	W-(eV)	W+(eV)
1	8	0.0001	0.0006	0.0004	0.0005	0	0.0001	0.0004
2	8	0	0	0	0	0	0	0
3	8	0.9677	0.3337	0.6507	-0.634	0.2411	0.6593	0.2274
4	8	0	0.0001	0	0	0	0	0
5	8	0	0	0	0	0	0	0
6	7	0.0059	0.0105	0.0082	0.0046	0.0016	0.004	0.0072
7	6	0.0007	0.0049	0.0028	0.0041	0.0003	0.0005	0.0033
8	6	0.0111	0.0063	0.0087	-0.0047	0.0028	0.0075	0.0043
9	6	0.0001	0.0012	0.0007	0.0012	0	0	0.0008
10	6	0.0001	0.0017	0.0009	0.0015	0.0001	0.0001	0.0011
11	6	0.0002	0.001	0.0006	0.0008	0.0001	0.0001	0.0007
12	6	0.0105	0.6312	0.3208	0.6207	0.0125	0.0071	0.43
13	6	0.0007	0.0012	0.001	0.0006	0.0002	0.0005	0.0008
14	6	0.0004	0.0014	0.0009	0.001	0.0001	0.0003	0.001
15	6	0.0001	0.0006	0.0003	0.0005	0	0.0001	0.0004
16	6	0.0015	0.003	0.0023	0.0015	0.0004	0.001	0.0021
17	1	0	0	0	0	0	0	0
18	1	0	0	0	0	0	0	0
19	1	0	0	0	0	0	0	0
20	1	0	0	0	0	0	0	0
21	1	0	0	0	0	0	0	0
22	1	0	0	0	0	0	0	0
23	1	0	0.0003	0.0001	0.0003	0	0	0.0002
24	1	0	0	0	0	0	0	0
25	1	0.0002	0.0001	0.0001	-0.0001	0	0.0001	0
26	1	0	0.0001	0.0001	0.0001	0	0	0.0001
27	1	0	0	0	0	0	0	0
28	1	0.0003	0.0001	0.0002	-0.0002	0.0001	0.0002	0.0001
29	1	0	0	0	0	0	0	0
30	1	0	0.0001	0.0001	0.0001	0	0	0.0001
31	1	0	0	0	0	0	0	0
32	1	0	0	0	0	0	0	0
33	6	0.0002	0.001	0.0006	0.0008	0.0001	0.0001	0.0007
34	9	0	0	0	0	0	0	0
35	1	0	0.0007	0.0003	0.0007	0	0	0.0004
36	9	0	0.0001	0	0.0001	0	0	0

5. Conclusions

Vitamin B5 and its virtually designed derivatives were selected for in-silico investigations. Utilizing the DFT/B3LYP method with 6–311G (d,p) basis set, the optimized geometry, atomic charges, chemical reactivity parameters, and natural bond calculations were performed. The energy gap calculated from the FMO's has a lower value of 2.257 eV and this indicates low kinetic stability and high biological activity of the compounds under study. Chemical descriptors analysis showed the higher chemical stability of Vit B5 CH=CF2. The result of the ADMET analysis proved good drug likeness and excellent ADME properties as well as permissible toxicity assessment. The molecular docking studies suggests that ligands Vit B5-CH=CF2 and Vit B5-CCl3 have the good binding affinity against the target cyclophilin A. These two Vitamin B5 derivatives demonstrated comparable anticancer effect when compared to known CypA inhibitors, as indicated by binding energy values (-5.861 and -5.478 kcal/mol) respectively. To conclude, the derivatives Vit B5-CH=CF2 and Vit B5-CCl3 are safe and feature a successful combination therapy as a pharmaceutical medicine and could be developed as efficient antiviral, antibacterial, and anticancer drugs.

ACKNOWLEDGEMENT

References

[1] M. Hrubša,T.Siatka,I.Nejmanová, M. Vopršalová, Kujovská L. Krčmová, K.Matoušová, & OEMONOM. Biological properties of vitamins of the B-Complex, part 1: vitamins B1, B2, B3, and B5. Nutrients, 14(3) (2022) 484.

[2] E. Premalatha, R. Dineshraj, I. Kannan, K.S. Bhaarath, & T.K.V. Sharavanan Molecular docking study on quercetin derivatives as inhibitors of Pantothenate Synthetase (PanC) of Mycobacterium tuberculosis. Int. J. Res. Pharm. Sci, 11 (2020) 3684-3690.

[3] T. Sanvictores, S. Chauhan Vitamin B5 (Pantothenic Acid) [Updated 2022 Oct 12]. In: StatPearls [Internet]. Treasure Island (FL): StatPearls Publishing; 2022 Jan-. Available from: https://www.ncbi.nlm.nih.gov/books/NBK563233/

[4] H.M. Said Intestinal absorption of water-soluble vitamins in health and disease. The Biochemical journal, 437(3) (2011) 357–372. https://doi.org/10.1042/BJ20110326

[5] Y. Zhou , C.M. Park, C.W. Cho, & Y.S. Song Protective effect of pinitol against D-galactosamine-induced hepatotoxicity in rats fed on a high-fat diet. Bioscience, biotechnology, and biochemistry, 72(7) (2008)1657–1666. https://doi.org/10.1271/bbb.70473

[6] V.S. Slyshenkov, A.G. Moiseenok & L.Wojtczak Noxious effects of oxygen reactive species on energy-coupling processes in Ehrlich ascites tumor mitochondria and the protection by pantothenic acid. Free radical biology & medicine, 20(6) (1996) 793–800. https://doi.org/10.1016/0891-5849(95)02210-4

[7] H. Schittl, & N.Getoff, Radiation-induced antitumor properties of vitamin B5 (pantothenic acid) and its effect on mitomycin C activity: experiments in vitro. Oncology research, 16(8) (2007) 389–394. https://doi.org/10.3727/000000006783980919

[8] V.S. Slyshenkov, K. Piwocka, E. Sikora, & L. Wojtczak. Pantothenic acid protects jurkat cells against ultraviolet light-induced apoptosis. Free radical biology & medicine, 30(11) (2001) 1303–1310. https://doi.org/10.1016/s0891-5849(01)00531-7

[9] P.N. Moorthy, E. Hayon: One electron redox reaction of water soluble vitamins. 4. thiamin (vit.B1), biotin and pantothenic acid. J Organ Chem 42 (1997) 879-885.

[10] H. Schittl, R.M. Quint, N.Getoff. Products of aqueous vitamin B5 (pantothenic acid) formed by free radical reactions. RadiatPhysChem 76 (200) 1594-1599.

[11] A.M. Deghady, R.K. Hussein, A.G. Alhamzani, &A. Mera. Density functional theory and molecular docking investigations of the chemical and antibacterial activities for 1-(4-hydroxyphenyl)-3-phenylprop-2-en-1-one. Molecules, 26(12) (2021) 3631.

[12] S. Liu, Y. Li, W. Wei, K. Wang, L. Wang, & J. Wang. Design, synthesis, molecular docking studies and anti-HBV activity of

phenylpropanoid derivatives. Chemico-Biological Interactions, 251 (2016) 1-9.

[13] F.F. Wang, W. Yang, Y.H. Shi, &G.W. Le. Molecular determinants of thyroid hormone receptor selectivity in a series of phosphonic acid derivatives: 3D-QSAR analysis and molecular docking. Chemico-biological interactions, 240 (2015) 324-335.

[14] F. A. Opo, M. M. Rahman, F. Ahammad, I. Ahmed, M. A. Bhuiyan, & A. M. Asiri. Structure based pharmacophore modeling, virtual screening, molecular docking and ADMET approaches for identification of natural anti-cancer agents targeting XIAP protein. Scientific reports, 11(1) (2021) 1-17.

[15] G. Vistoli, A. Pedretti, B. Testa. Assessing drug-likeness–what are we missing?. Drug discovery today, 13(7-8) (2008) 285-294.

[16] K. H. Ibnaouf, R. K. Hussein, Elkhair, & A. O. Elzupir. Experimental and theoretical study of the structure, frontier molecular orbital, tautomerism and spectral analysis of 3-(p-substituted phenyl)-5-phenyl-1H-pyrazole. Journal of Molecular Liquids, 287 (2019) 110675.

[17] A. M. Farag, A. M. Fahim.Synthesis, biological evaluation and DFT calculation of novel pyrazole and pyrimidine derivatives. Journal of Molecular Structure, 1179 (2019) 304-314.

[18] P. Nigro, G. Pompilio, M. C. Capogrossi. Cyclophilin A: a key player for human disease. Cell death & disease, 4(10) (2013) e888.

[19] X. Liu, L. Sun, M. Yu, Z. Wang, C. Xu, Q. Xue, K. Zhang, X. Ye, Y. Kitamura, W. Liu. Cyclophilin A interacts with influenza A virus M1 protein and impairs the early stage of the viral replication. Cellular microbiology, 11(5) (2009) 730–741.

[20] C. Luo, H. Luo, S. Zheng, C. Gui, L. Yue, C. Yu, T. Sun, P. He, J. Chen, J. Shen, X. Luo, Y. Li, H. Liu, D. Bai, J. Shen, Y. Yang, F. Li, J. Zuo, R. Hilgenfeld, G. Pei, H. Jiang. Nucleocapsid protein of SARS coronavirus tightly binds to human cyclophilin A. Biochemical and biophysical research communications, 321(3) (2004) 557–565.

[21] A. Hoerauf, C. Rascher, R. Bang, A. Pahl, W. Solbach, K. Brune, M. Röllinghoff & H. Bang. Host-cell cyclophilin is important for the intracellular replication of Leishmania major. Molecular microbiology, 24(2) (1997) 421–429.

[22] A. Bell, P. Monaghan, & A. P. Page. Peptidyl-prolyl cis-trans isomerases (immunophilins) and their roles in parasite biochemistry, host-parasite interaction and antiparasitic drug action. International journal for parasitology, 36(3) (2006) 261–276. https://doi.org/10.1016/j.ijpara.2005.11.003

[23] M. Dutta, P. Delhi, K. M. Sinha, R. Banerjee, & A. K. Datta. Lack of abundance of cytoplasmic cyclosporin A-binding protein renders free-living Leishmania donovani resistant to cyclosporin A. The Journal of biological chemistry, 276(22) (2001) 19294–19300. https://doi.org/10.1074/jbc.M009379200

[24] M. Berriman, & A. H. Fairlamb. Detailed characterization of a cyclophilin from the human malaria parasite Plasmodium falciparum. The Biochemical journal, 334 (2) (1998) 437–445. https://doi.org/10.1042/bj3340437

[25] H. Golding, J. Aliberti, L. R. King, J. Manischewitz, J. Andersen,, J. Valenzuela, N. R. Landau, & A. Sher. Inhibition of HIV-1 infection by a CCR5-binding cyclophilin from Toxoplasma gondii. Blood, 102(9) (2003) 3280–3286.

[26] H. Yang, J. Chen, J. Yang, S. Qiao, S. Zhao, & L. Yu. Cyclophilin A is upregulated in small cell lung cancer and activates ERK1/2 signal. Biochemical and biophysical research communications, 361(3) (2007) 763–767.

[27] Y. J. Qi, Q. Y. He, Y. F. Ma, Y. W. Du, G. C. Liu, Y. J. Li, G. S. Tsao, S. M. Ngai, & J. F. Chiu. Proteomic identification of malignant transformation-related proteins in esophageal squamous cell carcinoma. Journal of cellular biochemistry, 104(5) (2008) 1625–1635.

[28] B. A. Howard, R. Furumai, M. J. Campa, Z. N. Rabbani, Z. Vujaskovic, X. F. Wang, & E. F. Patz, Jr. Stable RNA interference-mediated suppression of cyclophilin A diminishes non-small-cell lung tumor growth in vivo. Cancer research, 65(19) (2005) 8853–8860.

[29] Z. Li, X. Zhao, S. Bai, Z. Wang, L. Chen, Y. Wei, & C. Huang. Proteomics identification of cyclophilin a as a potential prognostic factor and therapeutic target in endometrial carcinoma. Molecular & cellular proteomics: MCP, 7(10) (2008) 1810–1823.

[30] S. Semba, & K. Huebner. Protein expression profiling identifies cyclophilin A as a molecular target in Fhit-mediated tumor suppression. Molecular cancer research : MCR, 4(8) (2006) 529–538. https://doi.org/10.1158/1541-7786.MCR-06-0060 (Retraction published Mol Cancer Res. 2021 Apr;19(4):740).

[31] K. J. Choi, Y. J. Piao, M. J. Lim, J. H. Kim, J. Ha, W. Choe & S. S. Kim. Overexpressed cyclophilin A in cancer cells renders resistance to hypoxia- and cisplatin-induced cell death. Cancer research, 67(8) (2007) 3654–3662.

[32] C. C. Calhoun, Y. C. Lu, J. Song & R. Chiu. Knockdown endogenous CypA with siRNA in U2OS cells results in disruption of F-actin structure and alters tumor phenotype. Molecular and cellular biochemistry, 320 (1-2) (2009) 35–43.

[33] D. Cecconi, M. Donadelli, A. Scarpa, A. Milli, M. Palmieri, M. Hamdan, L. B. Areces, J. Rappsilber & P. G. Righetti. Proteomic analysis of pancreatic ductal carcinoma cells after combined treatment with gemcitabine and trichostatin A. Journal of proteome research, 4(6) (2005) 1909–1916.

[34] J. Lou, N. Fatima, Z. Xiao, S. Stauffer, G. Smythers, P. Greenwald & I. U. Ali. Proteomic profiling identifies cyclooxygenase-2-independent global proteomic changes by celecoxib in colorectal cancer cells. Cancer epidemiology, biomarkers &prevention : a publication of the American Association for Cancer Research, cosponsored by the American Society of Preventive Oncology, 15(9) (2006) 1598–1606.

[35] X. Han, S. H. Yoon, Y. Ding, T. G. Choi, W. J. Choi., H. Kim, Y. J. Kim, Y. B. Huh, J. Ha & S. S. Kim. Cyclosporin A and sanglifehrin A enhance chemotherapeutic effect of cisplatin in C6 glioma cells. Oncology reports, 23(4) (2010) 1053–1062.

[36] R. H. Hertwig, & W. Koch. On the parameterization of the local correlation functional. What is Becke-3-LYP?. Chemical Physics Letters, 268 (5-6) (1997) 345-351.

[37] K. Raghavachari. Perspective on "Density functional thermochemistry. III. The role of exact exchange". Theoretical Chemistry Accounts, 103(3) (2000) 361-363.

[38] M. J. E. A. Frisch, G. Trucks, H. B. Schlegel, G. E. Scuseria, M. A. Robb, J. R. Cheeseman & A. D. Fox. (2009). Gaussian 09, revision D. 01.

[39] R. Dennington, T. Keith, & J. G. Millam. (2009). Ver. 5. Semichem Inc.: Shawnee Mission, KS, USA.

[40] R. G. Parr. Density functional theory of atoms and molecules. In Horizons of quantum chemistry (pp. 5-15). (1980) Springer, Dordrecht.

[41] W. Yang, & R. G. Parr. Hardness, softness, and the fukui function in the electronic theory of metals and catalysis. Proceedings of the National Academy of Sciences, 82(20) (1985) 6723-6726.

[42] R. G. Parr, R. A. Donnelly, M. Levy & W. E. Palke. Electronegativity: the density functional viewpoint. The Journal of Chemical Physics, 68(8) (1978) 3801-3807.

[43] G. M. Morris, R. Huey, W. Lindstrom, M. F. Sanner, R. K. Belew, D. S. Goodsell, & A. J. Olson. AutoDock4 and AutoDockTools4: Automated docking with selective receptor flexibility. Journal of computational chemistry, 30(16) (2009) 2785-2791.

[44] D. S. Biovia. Discovery studio modeling environment (2017).

[45] A. Daina, O. Michielin, & V. Zoete. SwissADME: a free web tool to evaluate pharmacokinetics, drug-likeness and medicinal chemistry friendliness of small molecules. Scientific reports, 7(1) (2017) 1-13.

[46] R. K. Hussein, H. M. Elkhair, A. O. Elzupir, & K. H. Ibnaouf. Spectral, Structural, Stability Characteristics and Frontier Molecular Orbitals of tri-n-butyl phosphate (tbp) and its Degradation Products: DFT calculations. J. Ovonic Res, 17 (2021) 23-30.

[47] T. Tsuneda, J. W. Song, S. Suzuki, & K. Hirao. On Koopmans' theorem in density functional theory. The Journal of chemical physics, 133(17) (2010) 174101.

[48] T. L. Davis, J. R. Walker, V. Campagna-Slater, P. J. Finerty Jr, R. Paramanathan, et al. Structural and Biochemical Characterization of the Human Cyclophilin Family of Peptidyl-Prolyl Isomerases. PLoS Biol 8(7) (2010) e1000439.

[49] A. Mohebbi, A. Mirarab, R. Shaddel, M. Shafaei Fallah, A. Memarian. Molecular Dynamic Simulation and Docking of Cyclophilin A Mutants with its Potential Inhibitors. Journal of Clinical and Basic Research, (2) (2021) 26-41

[50] A. Mohebbi, A. Mirarab, R. Shaddel, M. Shafaei Fallah, A. Memarian. Molecular Dynamic Simulation and Docking of Cyclophilin A Mutants with its Potential Inhibitors. Journal of Clinical and Basic Research, (2) (2021) 26-41

[51] B. C. Doak, & J. Kihlberg. Drug discovery beyond the rule of 5-Opportunities and challenges. Expert Opinion on Drug Discovery, 12(2) (2017) 115-119.

[52] Q. S. Obu, H. Louis, J. O. Odey, I. J. Eko, S. Abdullahi, T. N. Ntui, & O. E. Offiong. Synthesis, spectra (FT-IR, NMR) investigations, DFT study, in silico ADMET and Molecular docking analysis of 2-amino-4-(4-aminophenyl) thiophene-3-carbonitrile as a potential anti-tubercular agent. Journal of Molecular Structure, 1244 (2021) 130880.

[53] I. Salim Meeran, V. Baskar, S. Syed Tajudeen, T. K. Shabeer. Design, ADME profiling, and molecular docking simulation of new isoniazid-Schiff base analogs as MtKasB inhibitors. Asian J. Res. Chem. Pharmaceut. Sci., 6(1) (2018) 20–34.

[54] A. Avdeef. Prediction of aqueous intrinsic solubility of druglike molecules using Random Forest regression trained with Wiki-pS0 database. ADMET and DMPK, 8(1) (2020) 29-77.

[55] C. P. Chen, C. C. Chen, C. W. Huang, & Y. C. Chang. Evaluating molecular properties involved in transport of small molecules in stratum corneum: A quantitative structure-activity relationship for skin permeability. Molecules, 23(4) (2018) 911.

[56] M. Gerardo-Ramírez, F. L. Keggenhoff, V. Giam, D. Becker, M. Groth, N. Hartmann, & M. Hartmann. CD44 Contributes to the Regulation of MDR1 Protein and Doxorubicin Chemoresistance in Osteosarcoma. International Journal of Molecular Sciences, 23(15) (2022) 8616.

[57] C. Kwok, P. A. Weller, S. Guioli, J. W. Foster, S. Mansour, O. Zuffardi, H. H. Punnett, M. A. Dominguez-Steglich, J. D. Brook, I. D. Young, et al. Mutations in SOX9, the gene responsible for Campomelic dysplasia and autosomal sex reversal. Am J Hum Genet. 57(5) (1995) 1028-36. PMID: 7485151; PMCID: PMC1801368.

[58] M. Dean, K. Moitra, & R. Allikmets. The human ATP-binding cassette (ABC) transporter superfamily. Human Mutation, 43(9) (2022) 1162-1182.

[59] J. Yu, Z. Zhou, J. Tay-Sontheimer, R. H. Levy, & I. Ragueneau-Majlessi. Intestinal drug interactions mediated by OATPs: a systematic review of preclinical and clinical findings. Journal of pharmaceutical sciences, 106(9) (2017) 2312-2325.

[60] S. Wolking, E. Schaeffeler, H. Lerche, M. Schwab & A. T. Nies. Impact of genetic polymorphisms of ABCB1 (MDR1, P-glycoprotein) on drug disposition and potential clinical implications: update of the literature. Clinical pharmacokinetics, 54(7) (2015) 709-735.

[61] R. Meenashi, K. Selvaraju, A. D. Stephen & C. Jelsch. Theoretical crystal structure prediction of aminosalicylic acid: Charge density topological and electrostatic analyses. Journal of Molecular Structure, 1213 (2020) 128139.

[62] L. S. Ghomi, M. Behzad, A. Tarahhomi & A. Arab. Crystal structures, DFT calculations, and Hirshfeld surface analyses of two new copper (II) and nickel (II) Schiff base complexes derived from meso-1, 2-diphenyl-1, 2-ethylenediamine. Journal of Molecular Structure, 1150 (2017) 214-226.

[63] M. A. Spackman & J. J. McKinnon. Fingerprinting intermolecular interactions in molecular crystals. CrystEngComm, 4(66) (2002) 378-392.

[64] P. Rajesh, P. Kandan, S. Sathish, A. Manikandan, S. Gunasekaran, T.

Gnanasambandan, & S. B. Abirami. Vibrational spectroscopic, UV–Vis, molecular structure and NBO analysis of Rabeprazole. Journal of Molecular Structure, 1137 (2017) 277-291.